



Published in final edited form as:

Curr Opin Pharmacol. 2023 October ; 72: 102364. doi:10.1016/j.coph.2023.102364.

Illuminating GPCR Signaling Mechanisms by NMR Spectroscopy with Stable-Isotope Labeled Receptors

Beining Jin,

Naveen Thakur,

Anuradha V. Wijesekara,

Matthew T. Eddy

Department of Chemistry; University of Florida; Gainesville, FL, 32611; USA

Abstract

G protein-coupled receptors (GPCRs) exhibit remarkable structural plasticity, which underlies their capacity to recognize a wide range of extracellular molecules and interact with intracellular partner proteins. Nuclear magnetic resonance (NMR) spectroscopy is uniquely well-suited to investigate GPCR structural plasticity, enabled by stable-isotope “probes” incorporated into receptors that inform on structure and dynamics. Progress with stable-isotope labeling methods in Eukaryotic expression systems has enabled production of native or nearly-native human receptors with varied and complementary distributions of NMR probes. These advances have opened up new avenues for investigating the roles of conformational dynamics in signaling processes, including by mapping allosteric communication networks, understanding the specificity of GPCR interactions with partner proteins and exploring the impact of membrane environments on GPCR function.

Introduction

G protein-coupled receptors (GPCRs) are sensory integral membrane proteins that recognize an enormous range of extracellular stimuli and interact with numerous intracellular partner proteins to initiate cellular signaling events. It is widely appreciated that the functions of GPCRs are enabled by their inherent structural plasticity, i.e., conformational dynamics, and a complete view of GPCR function must also include knowledge of their dynamic behavior [1,2]. While crystallography and cryo-EM have made tremendous progress determining GPCR structures, concurrently, great advances investigating conformational dynamics of GPCRs have been made by spectroscopic methods, especially nuclear magnetic resonance (NMR) spectroscopy [3]. Indeed, current understanding of GPCR molecular recognition mechanisms are highly informed from NMR studies [3].

NMR spectroscopy provides several significant advantages for studying GPCR conformational dynamics, including that experiments can be carried out at physiological

Corresponding author: Eddy, Matthew T (matthew.eddy@ufl.edu).

Conflict of interest statement

None declared

temperatures, do not require bulky tags, and frequently utilize proteins with native or nearly-native amino acid sequences. Importantly, NMR data provide information on GPCR structures and dynamics at the level of individual nuclei. This unique capability is enabled by stable-isotopes, which act as “probes” that sense changes in local structure, dynamics, and environments. By distributing NMR probes throughout the receptor, one can obtain a global view of GPCR conformational dynamics at atomic resolution. With advances in stable-isotope labeling approaches, inroads have been made into NMR studies with more challenging proteins, including GPCRs.

This review surveys stable-isotope labeling approaches for NMR studies of GPCRs, emphasizing methods that utilize NMR-observable nuclei other than ^{19}F , i.e., ^{13}C , ^{15}N , ^2H , and ^1H . ^{19}F -NMR complements experiments with these nuclei, as reviewed elsewhere [4,5]. Examples from the literature are presented that illustrate a range of expression systems for producing GPCRs and various methods for incorporating NMR probes, including stable-isotope labeling via chemical modification and via biosynthetic approaches. We discuss how advances in stable-isotope labeling and production of GPCRs have led to a more complete view of their functions by providing insights from NMR into GPCR-drug interactions, interactions with partner proteins, and impacts of the cellular environment on GPCR structure and conformational dynamics.

Overview of stable-isotope labeling approaches for NMR

Table 1 presents a survey from the literature of GPCRs expressed for NMR studies, employed expression systems, stable-isotope labeling schemes and employed membrane mimetics. GPCR NMR studies have used two general approaches for incorporating stable-isotope labels: post-translational chemical modification, especially reductive methylation of lysines, or incorporation via biosynthesis during protein expression. The majority of GPCR NMR studies have employed Eukaryotic expression systems, with insect cells (Sf9) being the most widely used organism. Most studies incorporated stable-isotopes via biosynthesis rather than chemical modification. To date, studies in solution have used mostly detergent micelles as membrane mimetics and have exclusively focused on class A GPCRs.

Studies of GPCR complexes with small molecules

A central question in GPCR signaling is how information from ligand binding at the orthosteric pocket is transmitted ~ 30 Å to the intracellular surface of the receptor. NMR studies covering a growing number of class A GPCRs have provided insight into allosteric transmission processes.

The adenosine $\text{A}_{2\text{A}}$ receptor, $\text{A}_{2\text{A}}\text{AR}$, a class A GPCR that regulates dopamine release and myocardial blood flow, has been the focus of multiple NMR studies. Expression of $\text{A}_{2\text{A}}\text{AR}$ in *Pichia pastoris* enabled uniform incorporation of stable-isotopes and extensive deuteration. This allowed highly resolved NMR spectra to be recorded that provided a global view of $\text{A}_{2\text{A}}\text{AR}$ structural plasticity. 2D [^{15}N , ^1H]-transverse relaxation-optimized spectroscopy (TROSY) [40] spectra of $\text{A}_{2\text{A}}\text{AR}$ revealed the impact of drugs and mutations to receptor hot spots on signal transduction (Figure 1, a and b) [7].

The same methodology was employed to study A_{2A}AR complexes with partial agonists [9], leading to the observation of conformations for highly conserved residues Trp^{6.48} and Phe^{6.44} unique from those observed in full agonist complexes (superscripts denote Ballesteros-Weinstein nomenclature). Extrinsic tryptophans were introduced using the same expression methodology to provide novel, well-dispersed ¹⁵N-¹H indole signals, which showed different responses at helices V, VI, and VII correlating with changes in the efficacy of bound drugs and a ternary complex with bound agonist and polypeptide derived from the carboxy terminus of Gα_S [8]. 2D [¹³C,¹H]-HMQC spectra of uniformly deuterated A_{2A}AR with ¹H/¹³C-labels at isoleucine δ1 methyl groups enabled experiments correlating fast side chain motions with the efficacy of bound drugs and sodium concentration [6] (Figure 1, c and d).

Adrenergic receptors, targets of catecholamine neurotransmitters, are one of the most studied class A GPCR subfamilies. NMR studies of β₂AR have so far exclusively produced the receptor in insect cells and have utilized both chemical modification and biosynthesis stable-isotope labeling approaches. Early studies of the β₂AR labeled with ε-¹³CH₃-methionine observed functionally important conformational states not represented among available crystal or cryo-EM structures [20] and demonstrated how drug efficacy influenced the equilibrium of different conformational states [21]. Improvements in signal-to-noise of NMR experiments with β₂AR in lipid nanodiscs were obtained by substituting a selected set of amino acids with ²H-labeled amino acids in protein expression media also containing ε-¹³CH₃-methionine [22] or β-¹³CH₃-Alanine [23]. Paramagnetic relaxation enhancement (PRE) experiments with ¹⁵N,²H-leucine labeled β₂AR yielded a structural model of the agonist-bound receptor that significantly differed from available crystal structures [25] (Figure 1, e and f). NMR studies of the related β₁AR incorporated ¹⁵N,²H-valines throughout the protein, which enabled visualization of how drug binding altered allosteric networks [12] and characterization of distinct conformers and quantitative measurement of their rates of exchange [13].

NMR studies have identified significant differences among the energy landscapes of class A receptors and propensities for activating specific signaling pathways. Utilizing ε-¹³CH₃-methionine labeling, NMR studies of an α_{1A}AR receptor engineered for *E. coli* expression correlated chemical shifts with ligand efficacies and conformations of receptor microswitches [11]. Microswitches are conserved clusters of amino acids though to play important roles in allosteric transmission of drug binding, as reviewed elsewhere [41]. In contrast, NMR observations of M₂R containing ε-¹³CH₃-methionine observed no clear correlations between chemical shifts and the efficacy of bound drugs, suggesting a more complex energy landscape comprising multiple distinct receptor conformations [30]. Stable isotope labeling with ε-¹³CH₃-methionine in combination with reductive methylation of lysine residues [35] and ε-¹³CH₃-methionine in a deuterated background [34] were employed to investigate the effects of ligand pharmacology on μ-OR signaling bias. The intrinsically biased receptor ACKR3 was studied using ε-¹³CH₃-methionine labeling, correlating conformational changes in the extracellular ligand-binding pocket with changes in the intracellular β-arrestin-coupling region [28]. NMR studies of a growing number of class A receptors have provided additional insights (see Table 1).

Investigations of GPCR ternary complexes

NMR experiments have expanded on work with GPCR binary complexes with ligands to studies of ternary complexes with partner signaling proteins. Observations from NMR experiments have provided insights into mechanisms of partner protein recognition and allosteric modulation of partner protein complex formation on orthosteric ligand binding

Single domain antibodies, termed nanobodies, have been used as mimetics of G proteins to investigate GPCR complex formation with partner proteins by structural and biophysical techniques, including NMR spectroscopy [12,15,17,19,20,28,30,33,35,42]. [^1H , ^{15}N]-TROSY spectra of ^{15}N -valine labeled $\beta_1\text{AR}$ in complex with nanobody Nb80 revealed allosteric communication pathways from the receptor's intracellular surface to the orthosteric binding pocket [12]. $\beta_1\text{AR}$ labeled with $e\text{-}^{13}\text{CH}_3$ -methionine showed rigid receptor dynamics in a ternary complex with agonist and nanobody Nb6b9 compared to intermediate timescale motion for complexes with agonists alone [15]. A comparison of $e\text{-}^{13}\text{CH}_3$ -methionine labeled $\beta_1\text{AR}$ in complex with Nb80 and the engineered G_S protein, 'mini-Gs', showed highly similar responses of the receptor in both complexes (Figure 2, a and b) [17].

The structural basis for GPCR-G protein selectivity is not well understood. This problem was explored by NMR with reductively ^{13}C -methylated $\beta_2\text{AR}$ to investigate the structural determinants as to why $\beta_2\text{AR}$ preferentially forms complexes with G_S over G_i [19]. Significant chemical shift differences between complexes with G_S and G_i were observed for methylated lysine residues located on the intracellular loop 2 (ICL2) of $\beta_2\text{AR}$ (Figure 2, c and d) [19]. Interactions between $\beta_2\text{AR}$ ICL2 and G proteins were found to be important determinants for selectivity of G_S over G_i in signaling complexes [19].

Mechanisms of arrestin-receptor complex formation have also been investigated by NMR spectroscopy. Early studies of [$u\text{-}^{15}\text{N}$, ^2H]-arrestin-1 interaction with rhodopsin observed global structural changes of arrestin-1 upon complex formation and indicated arrestin adopted a dynamic conformational ensemble [43]. A critical step preceding arrestin recruitment is phosphorylation of the disordered receptor C-terminus. The impact of phosphorylation on the conformation of the $\beta_2\text{AR}$ C-terminus was studied using a segmentally [^{13}C , ^{15}N]-labelled C-terminus covalently attached to the unlabeled receptor TM region using intein chemistry (Figure 2, e and f) [24]. Phosphorylation of the $\beta_2\text{AR}$ C-terminus was found to bring the C-terminus proximate to the membrane surface in samples reconstituted in lipid nanodiscs, placing residues in the C-terminus closer to the TM core to facilitate arrestin binding simultaneously to both receptor regions [24].

GPCR-lipid interactions explored by NMR

Increasing evidence from experimental and computational studies highlight the critical impact of lipids on GPCR function both through specific receptor-lipid interactions and by changing the bulk physical properties of the membrane bilayer [44]. NMR studies are investigating these dual roles, utilizing membrane mimetics including lipid nanodiscs and vesicles.

Cholesterol has been thought to modulate GPCR activity both directly as an orthosteric ligand, as in the case with the class F receptor Smoothed [45], and as a potential allosteric modulator [46]. Earlier saturation-transfer NMR experiments showed β_2 AR associated preferentially with cholesterol over ergosterol [47]. The role of cholesterol hemisuccinate (CHS), a more soluble analog of cholesterol, has been investigated as a potential negative allosteric modulator of the β_1 AR (Figure 3, a–c) [14]. Pressure-dependent ^1H - ^{15}N TROSY spectra of the G protein binding-competent ^{15}N -valine-labelled β_1 AR complex in the presence and absence of CHS were collected. Combining high-pressure NMR with crystallography, the location of a cavity in the receptor structure was found to correlate with a cholesterol-binding pocket. The presence of CHS was thus shown to prevent this pocket from collapsing and to block conformational changes of activation microswitches [14].

Observations correlating higher abundance of specific lipids with higher expression of certain GPCRs in some cell types led to the hypothesis that organ-specific GPCR functions may be driven by lipid-receptor interactions. For example, docosahexaenoic acid (DHA) and arachidonic acid (ARA) make up ~14% of the total lipid content in the mammalian brain striatum where A_{2A} AR is also extensively expressed [48]. 2D HMQC spectra of $[[\alpha,\beta,\beta\text{-}^2\text{H},\text{methyl-}^{13}\text{C}]\text{Met},\text{u-}^2\text{H}] A_{2A}$ AR showed distinct changes for A_{2A} AR in nanodiscs with and without DHA, especially near the intracellular surface in TM3 and TM6 (Figure 3 d–f) [10]. These changes correlated with a significant increase in GTP uptake by G proteins in complex with A_{2A} AR in the same lipid compositions [10].

Conclusions and Outlook

NMR has provided insights into GPCR structural plasticity so far predominantly for class A receptors (Table 1). Future experiments will expand on these initial studies to include more class A subfamilies and additional classes, facilitating comparison of function-related dynamics among more receptors. Exploration of GPCR complex formation with partner proteins by NMR is at the early stages, but initial literature data hint at the promise of NMR to provide improved understanding of the roles of post-translational modifications and membranes in signaling complex formation. Potentially transient complexes difficult to capture by structural techniques, such as GPCR interactions with kinases, may be more amenable to investigation by NMR. Flexible regions involved in the formation of signaling complexes, including the receptor C-terminus, are accessible to NMR and can be independently expressed, stable-isotope labeled and covalently attached to receptor cores via chemical ligation methods [24,49].

An emerging area of research where NMR will likely play a key role are investigations of the impact of the cellular environment, especially lipid membranes, on GPCR structure-function relationships. A seemingly limitless range of membrane and membrane-mimicking environments is accessible to NMR, including micelles, bicelles, nanodiscs for experiments in aqueous solutions, and vesicles for experiments in solids. Integrating data from NMR with cryo-EM structures of receptors in membrane mimetics will likely be a powerful combination to address questions on receptor-lipid interactions, including the affinities of lipids for different structural regions. Ultimately, membrane mimetics may not even

be needed. The advent of technologies for enhancing the sensitivity of NMR, including dynamic nuclear polarization [50,51], promises to provide opportunities to study GPCRs directly *in situ* in their native cellular environments.

Acknowledgements

This work was supported by the National Institutes of Health grant R35GM138291.

References

- Gusach A, et al. : Beyond structure: Emerging approaches to study GPCR dynamics. *Curr Opin Struct Biol* 2020, 63:18–25. [PubMed: 32305785]
- Latorraca NR, Venkatakrisnan AJ, Dror RO: GPCR dynamics: Structures in motion. *Chem Rev* 2017, 117:139–155. [PubMed: 27622975]
- Shimada I, et al. : GPCR drug discovery: Integrating solution NMR data with crystal and cryo-em structures. *Nat Rev Drug Discov* 2019, 18:59–82. [PubMed: 30410121]
- Picard L-P, Prosser RS: Advances in the study of GPCRs by 19F NMR. *Curr Opin Struct Biol* 2021, 69:169–176. [PubMed: 34130235]
- Didenko T, et al. : Fluorine-19 NMR of integral membrane proteins illustrated with studies of GPCRs. *Curr Opin Struct Biol* 2013, 23:740–747. [PubMed: 23932201]
- Clark LD, et al. : Ligand modulation of sidechain dynamics in a wild-type human GPCR. *Elife* 2017, 6.** First report of ILV-labeled human GPCR produced in a deuterated background revealing fast dynamics induced by different bound ligands
- Eddy MT, et al. : Allosteric coupling of drug binding and intracellular signaling in the A_{2A} adenosine receptor. *Cell* 2018, 172:68–80. [PubMed: 29290469] ** NMR data of uniform ²H, ¹⁵N-labeled GPCR provided global view of the impact of drugs and mutations on activation hotspots and signal transduction
- Eddy MT, et al. : Extrinsic tryptophans as NMR probes of allosteric coupling in membrane proteins: Application to the A_{2A} adenosine receptor. *J Am Chem Soc* 2018, 140:8228–8235. [PubMed: 29874058]
- Eddy MT, Martin BT, Wuthrich K: A_{2A} adenosine receptor partial agonism related to structural rearrangements in an activation microswitch. *Structure* 2021, 29:170–176 e173. [PubMed: 33238145] ** Structural basis for partial agonism relating distinct conformation of activation hot spot to structural changes at receptor intracellular surface
- Mizumura T, et al. : Activation of adenosine A_{2A} receptor by lipids from docosahexaenoic acid revealed by NMR. *Sci Adv* 2020, 6:eaay8544. [PubMed: 32206717] * NMR study relating presence of specific lipids to changes in G protein activity for GPCR in lipid nanodiscs
- Wu FJ, et al. : Probing the correlation between ligand efficacy and conformational diversity at the α 1A-adrenoreceptor reveals allosteric coupling of its microswitches. *J Biol Chem* 2020, 295:7404–7417. [PubMed: 32303636]
- Isogai S, et al. : Backbone NMR reveals allosteric signal transduction networks in the β 1-adrenergic receptor. *Nature* 2016, 530:237–241. [PubMed: 26840483] ** NMR data of ¹⁵N-valine labeled β 1AR show allosteric impact of partner protein binding on the GPCR orthosteric ligand pocket
- Grahl A, et al. : A high-resolution description of β 1-adrenergic receptor functional dynamics and allosteric coupling from backbone NMR. *Nat Commun* 2020, 11:2216. [PubMed: 32371991]
- Abiko LA, et al. : Filling of a water-free void explains the allosteric regulation of the β 1-adrenergic receptor by cholesterol. *Nat Chem* 2022, 14:1133–1141. [PubMed: 35953642] ** Integrating NMR data and crystallography to provide a structural basis for allosteric modulation of a receptor by cholesteryl hemisuccinate
- Solt AS, et al. : Insight into partial agonism by observing multiple equilibria for ligand-bound and Gs-mimetic nanobody-bound β 1-adrenergic receptor. *Nat Commun* 2017, 8:1795. [PubMed: 29176642]

16. Opitz C, Isogai S, Grzesiek S: An economic approach to efficient isotope labeling in insect cells using homemade ^{15}N -, ^{13}C - and ^2H -labeled yeast extracts. *J Biomol NMR* 2015, 62:373–385. [PubMed: 26070442]
17. Rossler P, et al. : GPCR activation states induced by nanobodies and mini-G proteins compared by NMR spectroscopy. *Molecules* 2020, 25.
18. Bokoch MP, et al. : Ligand-specific regulation of the extracellular surface of a G-protein-coupled receptor. *Nature* 2010, 463:108–112. [PubMed: 20054398]
19. Ma X, et al. : Analysis of $\beta_2\text{AR}$ -Gs and $\beta_2\text{AR}$ -Gi complex formation by NMR spectroscopy. *Proc Natl Acad Sci U S A* 2020, 117:23096–23105. [PubMed: 32868434] ** Structural basis for $\beta_2\text{AR}$ G protein selectivity determined to involve key residues in intracellular loop 2.
20. Nygaard R, et al. : The dynamic process of β_2 -adrenergic receptor activation. *Cell* 2013, 152:532–542. [PubMed: 23374348]
21. Kofuku Y, et al. : Efficacy of the β_2 -adrenergic receptor is determined by conformational equilibrium in the transmembrane region. *Nat Comm* 2012, 3:1045.
22. Kofuku Y, et al. : Functional dynamics of deuterated β_2 -adrenergic receptor in lipid bilayers revealed by NMR spectroscopy. *Angew Chem* 2014, 53:13376–13379. [PubMed: 25284766]
23. Kofuku Y, et al. : Deuteration and selective labeling of alanine methyl groups of β_2 -adrenergic receptor expressed in a baculovirus-insect cell expression system. *J Biomol NMR* 2018, 71:185–192. [PubMed: 29520682]
24. Shiraishi Y, et al. : Phosphorylation-induced conformation of β_2 -adrenoceptor related to arrestin recruitment revealed by NMR. *Nat Commun* 2018, 9:194. [PubMed: 29335412] * Structural basis for arrestin recruitment involved interactions of a phosphorylated receptor C-terminus with the surface of a membrane mimetic.
25. Imai S, et al. : Structural equilibrium underlying ligand-dependent activation of β_2 -adrenoreceptor. *Nat Chem Biol* 2020, 16:430–439. [PubMed: 31959965] ** NMR PRE experiments provided structural model of a GPCR bound to an agonist with significant differences from available crystal structures.
26. Casiraghi M, et al. : Functional modulation of a G protein-coupled receptor conformational landscape in a lipid bilayer. *J Am Chem Soc* 2016, 138:11170–11175. [PubMed: 27489943]
27. Yeliseev A: Expression and preparation of a G-protein-coupled cannabinoid receptor CB2 for NMR structural studies. *Curr Protoc Protein Sci* 2019, 96:e83. [PubMed: 30624864]
28. Kleist AB, et al. : Conformational selection guides β -arrestin recruitment at a biased G protein-coupled receptor. *Science* 2022, 377:222–228. [PubMed: 35857540] * NMR observations of β -arrestin recruitment to an atypical chemokine receptor by tuning receptor dynamics through bound ligands.
29. Mulry E, Ray AP, Eddy MT: Production of a human histamine receptor for NMR spectroscopy in aqueous solutions. *Biomolecules* 2021, 11.
30. Xu J, et al. : Conformational complexity and dynamics in a muscarinic receptor revealed by NMR spectroscopy. *Mol Cell* 2019, 75:53–65 e57. [PubMed: 31103421]
31. Goba I, et al. : Probing the conformation states of neurotensin receptor 1 variants by NMR site-directed methyl labeling. *ChemBioChem* 2021, 22:139–146. [PubMed: 32881260]
32. Bumbak F, et al. : Optimization and $^{13}\text{CH}_3$ methionine labeling of a signaling competent neurotensin receptor 1 variant for NMR studies. *Biochim Biophys Acta Biomembr* 2018, 1860:1372–1383. [PubMed: 29596791]
33. Sounier R, et al. : Propagation of conformational changes during mu-opioid receptor activation. *Nature* 2015, 524:375–378. [PubMed: 26245377]
34. Okude J, et al. : Identification of a conformational equilibrium that determines the efficacy and functional selectivity of the mu-opioid receptor. *Angew Chem* 2015, 54:15771–15776. [PubMed: 26568421]
35. Cong X, et al. : Molecular insights into the biased signaling mechanism of the mu-opioid receptor. *Mol Cell* 2021, 81:4165–4175 e4166. [PubMed: 34433090] *NMR data support structural basis for biased agonism of a GPCR through involvement of intracellular loops and helix 8.
36. Clark L, et al. : On the use of pichia pastoris for isotopic labeling of human GPCRs for NMR studies. *J Biomol NMR* 2018, 71:203–211. [PubMed: 30121871]

37. Stehle J, et al. : Characterization of the simultaneous decay kinetics of metarhodopsin states ii and iii in rhodopsin by solution-state NMR spectroscopy. *Angew Chem* 2014, 53:2078–2084. [PubMed: 24505031]
38. Pope AL, et al. : A conserved proline hinge mediates helix dynamics and activation of rhodopsin. *Structure* 2020, 28:1004–1013 e1004. [PubMed: 32470317]
39. Ahuja S, et al. : Helix movement is coupled to displacement of the second extracellular loop in rhodopsin activation. *Nat Struct Mol Biol* 2009, 16:168–175. [PubMed: 19182802]
40. Pervushin K, et al. : Attenuated t2 relaxation by mutual cancellation of dipole–dipole coupling and chemical shift anisotropy indicates an avenue to NMR structures of very large biological macromolecules in solution. *Proc. Natl. Acad. Sci. USA* 1997:6.
41. Katritch V, Cherezov V, Stevens RC: Structure-function of the G protein–coupled receptor superfamily. *Annu Rev Pharmacol Toxicol* 2013, 53:531–556. [PubMed: 23140243]
42. Manglik A, et al. : Structural insights into the dynamic process of β_2 -adrenergic receptor signaling. *Cell* 2015, 161:1101–1111. [PubMed: 25981665]
43. Zhuang T, et al. : Involvement of distinct arrestin-1 elements in binding to different functional forms of rhodopsin. *Proc Natl Acad Sci* 2013, 110:942–947. [PubMed: 23277586]
44. Jones AJY, et al. : Structure and dynamics of GPCRs in lipid membranes: Physical principles and experimental approaches. *Molecules* 2020, 25:4729. [PubMed: 33076366]
45. Luchetti G, et al. : Cholesterol activates the G-protein coupled receptor smoothed to promote hedgehog signaling. *eLife* 2016, 5:e20304. [PubMed: 27705744]
46. van der Westhuizen ET, et al. : Endogenous allosteric modulators of G protein–coupled receptors. *J Pharmacol Exp Ther* 2015, 353:246–260. [PubMed: 25650376]
47. Gater Deborah L, et al. : Two classes of cholesterol binding sites for the β_2 AR revealed by thermostability and NMR. *Biophys J* 2014, 107:2305–2312. [PubMed: 25418299]
48. Xiao Y, Huang Y, Chen Z-Y: Distribution, depletion and recovery of docosahexaenoic acid are region-specific in rat brain. *Brit J Nutr* 2005, 94:544–550. [PubMed: 16197579]
49. Li Y, et al. : Chemical synthesis of a full-length G-protein-coupled receptor β_2 -adrenergic receptor with defined modification patterns at the c-terminus. *J Am Chem Soc* 2021, 143:17566–17576. [PubMed: 34663067]
50. Su Y, Andreas L, Griffin RG: Magic angle spinning NMR of proteins: High-frequency dynamic nuclear polarization and ^1H detection. *Annu Rev Biochem* 2015, 84:465–497. [PubMed: 25839340]
51. Barnes AB, et al. : High-field dynamic nuclear polarization for solid and solution biological NMR. *Appl Mag Res* 2008, 34:237–263.

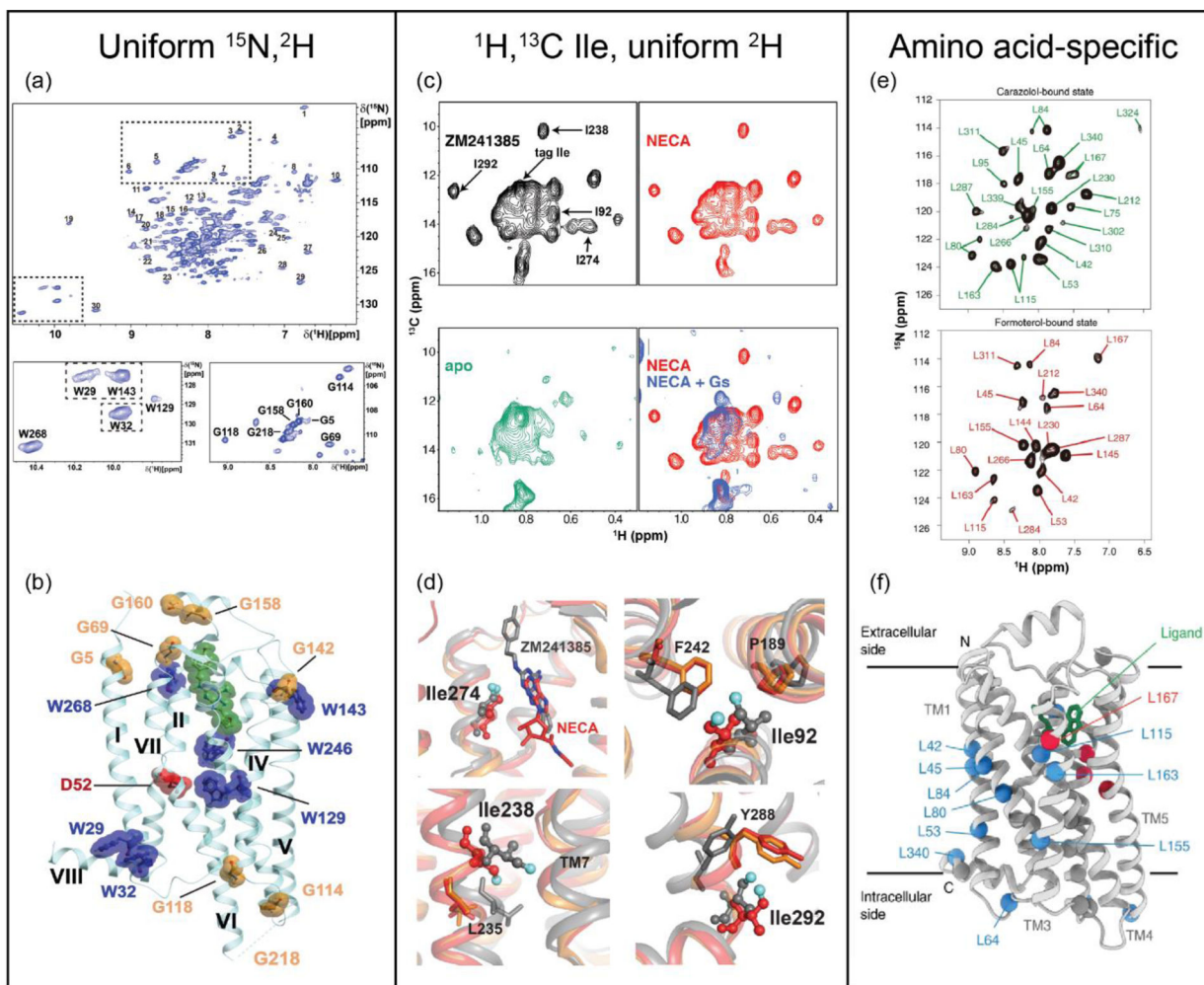


Figure 1.

Insights from NMR into ligand-stimulated GPCR activation. **(a)** 2D [^{15}N , ^1H]-TROSY spectrum of [$u\text{-}^{15}\text{N}$, $\sim 70\%$ ^2H]- $\text{A}_{2\text{A}}\text{AR}$ in complex with the antagonist ZM241385. Regions containing Trp indole ^{15}N - ^1H and Gly backbone signals are expanded. **(b)** Assigned signals mapped onto an $\text{A}_{2\text{A}}\text{AR}$ crystal structure (PDB 6AQF) with the antagonist ZM241385 shown in green and conserved residue Asp52 in red. **(c)** [^{13}C , ^1H]-HMQC spectra of several complexes of [^1H , ^{13}C -Ile $\delta 1$, $u\text{-}^2\text{H}$]- $\text{A}_{2\text{A}}\text{AR}$ with assigned signals annotated. **(d)** Superimposed crystal structures of $\text{A}_{2\text{A}}\text{AR}$ in complex with the antagonist ZM241385 (gray, PDB 4EIY), agonist NECA (red, PDB 2YDV), and agonist UK432097 (orange, PDB 3QAK), highlighting regions where significant chemical shift changes were observed. **(e)** 2D [^{15}N , ^1H]-TROSY correlation spectra of [$2,3,3\text{-}^2\text{H}$, ^{15}N Leu]- $\beta_2\text{AR}$ in complex with the antagonist carazolol and agonist formoterol. **(f)** Chemical shift differences observed between antagonist- and agonist-bound $\beta_2\text{AR}$ mapped onto the crystal structure of $\beta_2\text{AR}$ in complex with carazolol (PDB 2RH1); red spheres and blue spheres denote amide signals of leucine residues with chemical shift differences >0.4 ppm and <0.4 ppm, respectively. Panels **a** and **b** adapted from reference 7, panels **c** and **d** adapted from reference 6, and panels **e** and **f** adapted from reference 24, with permission.

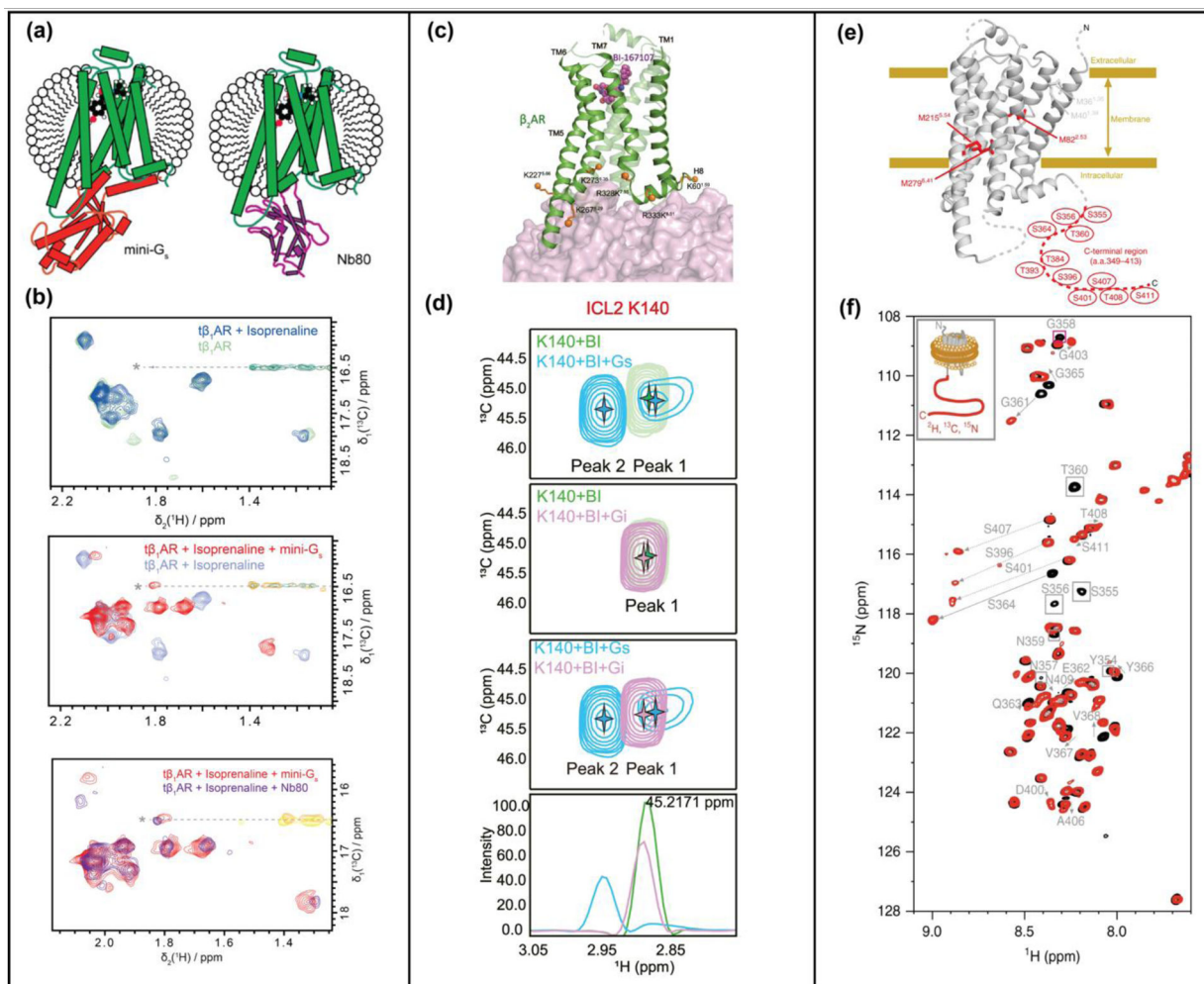


Figure 2.

NMR studies of GPCR ternary complexes. **(a)** Complexes of β_1 AR with an engineered Gs protein (mini-Gs) and G protein-mimicking nanobody, Nb80, compared by NMR. Schematics show β_1 AR ternary complexes with an agonist and mini-Gs or nanobody NB80. **(b)** Superimposed ^{13}C , ^1H -HMQC spectra of β_1 AR in complex with an agonist and in ternary complexes with either mini-Gs or Nb80. **(c)** β_2 AR-G protein interactions studied by reductive methylation of lysines. Lysines used as NMR probes are shown as orange solid spheres on the structure of the β_2 AR-Gs complex (PDB 3SN6). **(d)** Expanded panels from ^{13}C , ^1H -HSQC spectra of β_2 AR highlighting chemical shift differences of K140 between complexes with G_s and G_i, indicating involvement of ICL2 in differentiating G_s and G_i. **(e)** Phosphorylated β_2 AR and β_2 AR in complex with arrestin studied with ϵ - ^{13}C -methionine labeling and segmental labeling. **(f)** Superimposed ^{15}N , ^1H -HSQC spectra of β_2 AR (black) and phosphorylated β_2 AR (red) with segmentally-labeled C-terminus. Significant chemical shift changes are indicated with arrows. Panels **a** and **b** adapted from reference 17, **c** and **d** adapted from reference 19, and **e** and **f** adapted from reference 23, with permission.

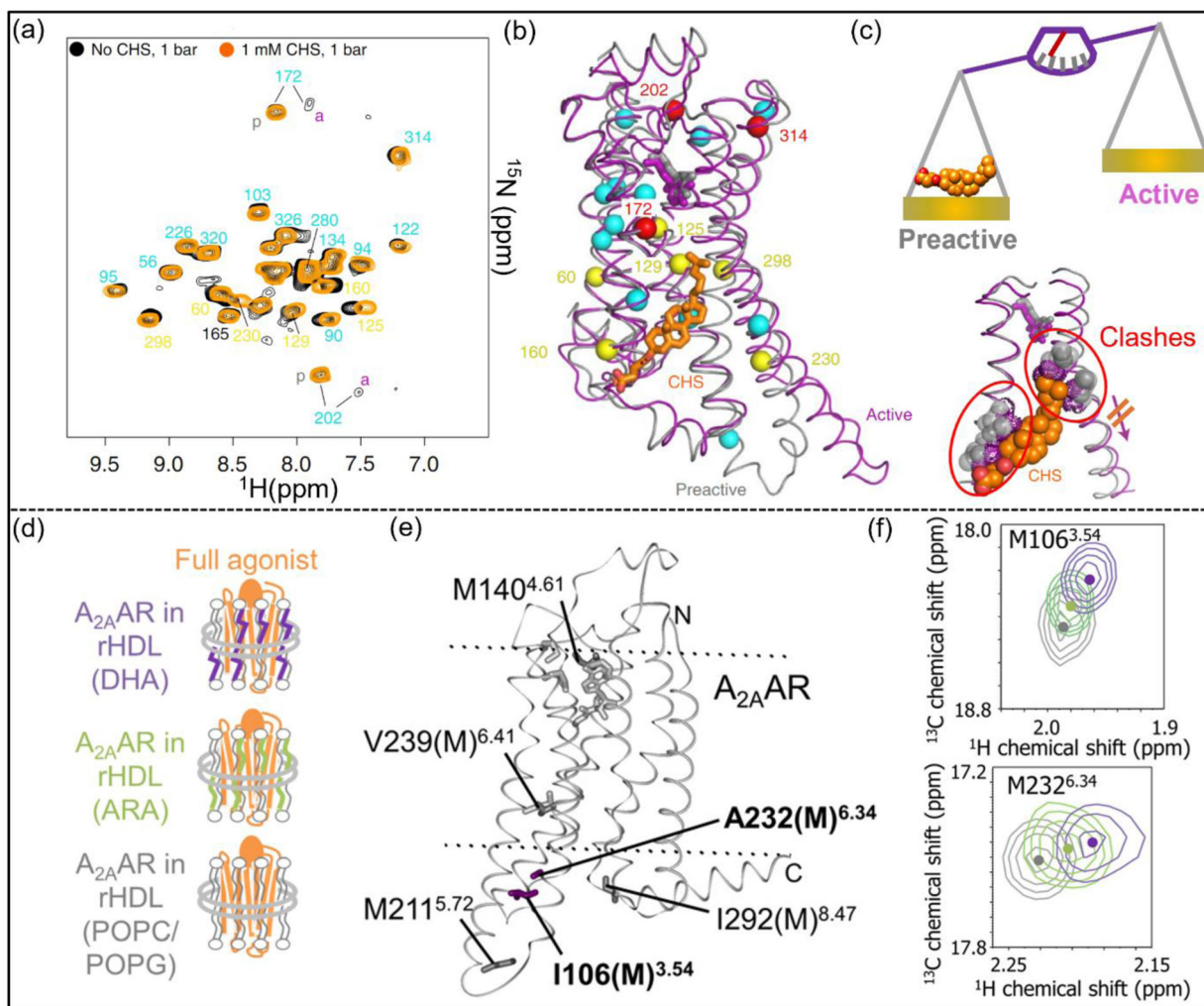


Figure 3. NMR investigations of membrane composition on GPCR function-related dynamics. **(a)** Superposition of [^{15}N , ^1H]-TROSY spectra of ^{15}N -valine $\beta_1\text{AR}$ in the absence (black) or presence (orange) of CHS. **(b)** Responses to CHS (orange sticks) mapped onto the crystal structures of pre-active (PDB 2Y03, grey) and active (PDB 6H7J, magenta) $\beta_1\text{AR}$. Valine ^{15}N - ^1H amides in **(a)** are shown as spheres colored by their response to CHS (red, increasing pre-active conformation population; yellow, moderate chemical shift change; cyan, small chemical shift change). **(c)** NMR data and crystal structures provided a view of CHS as a negative allosteric modulator of activation. **(d)** Schematics of $\text{A}_{2\text{A}}\text{AR}$ reconstituted in nanodiscs containing lipids and DHA or ARA. **(e)** ϵ - $^{13}\text{CH}_3$ -methionine used to monitor the receptor's response to DHA and ARA. I106(M) and A232(M) showed larger chemical shift differences and are shown as purple sticks. NECA and the less affected methionines are shown as grey sticks. **(f)** Signals for M106 and M232 in superimposed ^1H - ^{13}C HMQC spectra. Peak colors correspond to the colored text in **(d)**. Panels **a-c** adapted from reference 14, and panels **d-f** adapted from reference 10, with permission.

Table 1

GPCR	Expression system	Isotope labeling	Membrane Mimetic	Ref.
		ϵ - $^{13}\text{C}_3$ -Ile, ^2H	Detergent micelles	[6]
A _{2A} AR	Yeast (<i>P. pastoris</i>)	u - ^{15}N , ~70% ^2H	Detergent micelles	[7], [8], [9]
		ϵ - $^{13}\text{C}_3$ -Met	Lipid nanodiscs	[10]
α_{1A} AR	<i>E. coli</i>	ϵ - $^{13}\text{C}_3$ -Met	Detergent micelles	[11]
	Insect cells (<i>Sf9</i>)	^{15}N -Valine	Detergent micelles	[12], [13], [14]
β_1 AR		ϵ - $^{13}\text{C}_3$ -Met	Detergent micelles	[15]
	Insect cells (<i>Sf9</i>)	u - ^{15}N , >60% ^2H	Detergent micelles	[16]
	Mammalian cells	ϵ - $^{13}\text{C}_3$ -Met	Detergent micelles	[17]
		($^{13}\text{C}_3$)-Lys reductive dimethylation	Detergent micelles	[18], [19]
		ϵ - $^{13}\text{C}_3$ -Met	Detergent micelles	[20,21]
	Insect cells (<i>Sf9</i>)	ϵ - $^{13}\text{C}_3$ -Met, ^2H	Lipid nanodiscs	[22]
β_2 AR		β - $^{13}\text{C}_3$ -Ala, ^2H	Detergents micelles Lipid nanodiscs	[23]
	Insect cells (<i>Sf9</i>) and <i>E. coli</i>	ϵ - $^{13}\text{C}_3$ -Met, ^2H , c-term- ^2H , ^{13}C , ^{15}N	Lipid nanodiscs	[24]
		[2,3,3- ^2H , ^{15}N]-leucine	Detergent micelles	[25]
BLT ₂	<i>E. coli</i>	ϵ - $^{13}\text{C}_3$ -Met and ϵ - $^{13}\text{C}_3$ -Ile	Lipid nanodiscs	[26]
CB2	Yeast (<i>P. pastoris</i>)	ϵ - $^{13}\text{C}_3$ -Ile	Detergent micelles	[27]
ACKR3	Insect cells	ϵ - $^{13}\text{C}_3$ -Met	Detergent micelles	[28]
H ₁ R	Yeast (<i>P. pastoris</i>)	u - ^{15}N , ~70% ^2H	Detergent micelles	[29]
M ₂ R	Insect cells (<i>Sf9</i>)	ϵ - $^{13}\text{C}_3$ -Met	Detergent micelles	[30]
		^{13}C -MMTS	Detergent micelles	[31]
NTR1	<i>E. coli</i>	ϵ - $^{13}\text{C}_3$ -Met	Detergent micelles	[32]
		ϵ - $^{13}\text{C}_3$ -Met, ^2H	Detergent micelles	[33]
μ OR	Insect cells	($^{13}\text{C}_3$)-Lys reductive dimethylation	Detergent micelles	[34], [35]
OX ₂ R	Yeast (<i>P. pastoris</i>)	ϵ - $^{13}\text{C}_3$ -Ile	Detergent micelles	[36]
CB1	Yeast (<i>P. pastoris</i>)	ϵ - $^{13}\text{C}_3$ -Ile	Detergent micelles	[36]
		α , ϵ - ^{15}N -Trp		[37],[38]
Rhodopsin	Mammalian cells	$^{13}\text{C}\beta$ -Ser, $^{13}\text{C}\beta$ -Cys, $^{13}\text{C}\alpha$ -Gly	Detergent micelles	[39]

Abbreviations: A_{2A}AR, adenosine A_{2A} receptor; α_{1A} AR, α_{1A} -adrenergic receptor; β_1 AR, β_1 -Adrenergic receptor; β_2 AR, β_2 -Adrenergic receptor; BLT₂, leukotriene B₄ receptor 2; CB2, Cannabinoid receptor type 2; ACKR3, atypical chemokine receptor 3; H₁R, histamine H₁ receptor; M₂R, muscarinic acetylcholine receptor M₂; NTR1, neurotensin receptor type 1; μ OR, μ -opioid receptor; OX₂R, orexin receptor type 2; CB1, cannabinoid receptor type 1.